Integrin inhibitor suppresses bevacizumab-induced glioma invasion

Joji Ishida, Manabu Onishi, Kazuhiko Kurozumi, Tomotsugu Ichikawa, Kentaro Fujii, Yosuke Shimazu, Tetsuo Oka, Isao Date

Joji Ishida, Department of Neurological Surgery, Okayama University Graduate School of Medicine, Dentistry and Pharmaceutical Sciences, Okayama, Japan, 2-5-1 Shikata-Cho, Kita-ku Okayama 700-8558, JAPAN

Manabu Onishi, Department of Neurological Surgery, Okayama University Graduate School of Medicine, Dentistry and Pharmaceutical Sciences, Okayama, Japan, 2-5-1 Shikata-Cho, Kita-ku Okayama 700-8558, JAPAN

Kazuhiko Kurozumi, Department of Neurological Surgery, Okayama University Graduate School of Medicine, Dentistry and Pharmaceutical Sciences, Okayama, Japan, 2-5-1 Shikata-Cho, Kita-ku Okayama 700-8558, JAPAN

Tomotsugu Ichikawa, Department of Neurological Surgery, Okayama University Graduate School of Medicine, Dentistry and Pharmaceutical Sciences, Okayama, Japan, 2-5-1 Shikata-Cho, Kita-ku Okayama 700-8558, JAPAN

Kentaro Fujii, Department of Neurological Surgery, Okayama University Graduate School of Medicine, Dentistry and Pharmaceutical Sciences, Okayama, Japan, 2-5-1 Shikata-Cho, Kita-ku Okayama 700-8558, JAPAN

Yosuke Shimazu, Department of Neurological Surgery, Okayama University Graduate School of Medicine, Dentistry and Pharmaceutical Sciences, Okayama, Japan, 2-5-1 Shikata-Cho, Kita-ku Okayama 700-8558, JAPAN

Tetsuo Oka, Department of Neurological Surgery, Okayama University Graduate School of Medicine, Dentistry and Pharmaceutical Sciences, Okayama, Japan, 2-5-1 Shikata-Cho, Kita-ku Okayama 700-8558, JAPAN

Isao Date, Department of Neurological Surgery, Okayama University Graduate School of Medicine, Dentistry and Pharmaceutical Sciences, Okayama, Japan, 2-5-1 Shikata-Cho, Kita-ku Okayama 700-8558, JAPAN

Corresponding Author: Kazuhiko Kurozumi M.D., Ph.D.
Address: 2-5-1 Shikata-Cho, Kita-ku Okayama 700-8558, JAPAN,
Phon: +81-86-235-7336, FAX: +81-86-227-0191
E-mail: kkuro@md.okayama-u.ac.jp

Running title: The treatment for bevacizumab-induced glioma invasion

Keywords: glioma, invasion, bevacizumab, cilengitide, integrin.

Abstract

Glioblastoma is known to secrete high levels of vascular endothelial growth factor (VEGF), and clinical studies with bevacizumab, a monoclonal antibody to VEGF, have demonstrated convincing therapeutic benefits. However, its induction of invasive proliferation has also been reported. We examined the effects of treatment with cilengitide, an integrin inhibitor, on bevacizumab-induced invasive changes in glioma. U87ΔEGFR orthotopic rat and mouse models were treated by cilengitide and/or bevacizumab intraperitoneally. We analyzed brain tumors histopathologically about the three following groups: untreated, treated with bevacizumab, and treated with a combination of bevacizumab and cilengitide. Next, the combination group was compared to the bevacizumab monotherapy group using microarray analysis of extracted RNA from U87ΔEGFR brain tumors. Bevacizumab treatment led to increased cell invasion in spite of decreased angiogenesis. In the combination group, the depth of tumor invasion was significantly less than with only bevacizumab. Pathway analysis using the microarray data demonstrated the inhibition of invasion-associated genes such as the *integrin-mediated cell adhesion pathway* in the combination group. This study showed that the combination of bevacizumab with cilengitide exerted its anti-invasive effect by suppressing the *integrin-mediated cell adhesion pathway*. The elucidation of this mechanism might contribute to the treatment of bevacizumab-refractory glioma.

Introduction

Glioblastoma is one of the most frequent and aggressive intracranial neoplasms in humans and its prognosis remains poor despite the advancement of basic and clinical research. The median survival of patients diagnosed with glioblastoma is approximately 12–14 months [1]. The typical features of malignant glioma include aggressive proliferation, a strong invasive capacity, and extensive angiogenesis. Recently, new therapeutic agents such as various molecular targeted drugs have been developed and clinical trials have been conducted.

Glioblastoma cells are known to secrete high levels of vascular endothelial growth factor (VEGF), and clinical studies with the humanized monoclonal antibody bevacizumab, which targets the pro-angiogenic VEGF, have demonstrated significant therapeutic benefits in patients with recurrent glioblastoma [2-4]. Recently, the results of the positive phase III AVAglio and RTOG 0825 studies, which were presented at the 49th Annual American Society of Clinical Oncology (ASCO) Meeting in 2013, showed that bevacizumab in combination with radiation and temozolomide chemotherapy reduced the risk of progression-free survival in patients with newly diagnosed glioblastoma; however, overall survival did not reach statistical significance. Although anti-VEGF therapies including bevacizumab have been shown to decrease vascular permeability rapidly, which manifests as a decrease in contrast on enhanced magnetic resonance imaging, they do not improve the long-term outcome of patients [5]. Piao et al. showed that anti-VEGF therapy induces a phenotypic shift toward a more invasive, aggressive, and treatment-resistant phenotype associated with mechanisms similar to the epithelial to mesenchymal transition [6].

Integrins control the attachment of cells to the extracellular matrix (ECM) and participate in processes such as cell migration, differentiation, and survival during embryogenesis, angiogenesis, wound healing, and cellular defense against genotoxic assaults [7]. Several integrin-targeted drugs are in clinical trials as potential compounds for the treatment of cancer. Cilengitide (EMD121974), a cyclic arginine-glycine-aspartic (RGD) acid pentapeptide, is an αvβ3 and αvβ5 integrin antagonist that induces anoikis and apoptosis in human endothelial cells and brain tumor cells [8,9]. Cilengitide might inhibit adhesion to the ECM, thereby suppressing the invasion of glioma [10]. This agent is currently being assessed in phase III trials for glioblastoma patients and phase II trials for other types of cancers, with promising therapeutic outcomes reported to date [11].

The purpose of this study was to investigate the phenotypic changes in radiographic tumor progression that have been observed in some patients receiving bevacizumab. We

found that anti-VEGF treatment led to perivascular and subpial tumor invasion. Moreover, we investigated the pathological and molecular changes of the anti-angiogenic and anti-invasive effects using combination therapy of bevacizumab and the integrin antagonist cilengitide.

Materials and Methods

Glioma cell line and drug

The human glioma cell line U87ΔEGFR was seeded in tissue culture dishes (BD Falcon, Franklin Lakes, NJ, USA) and cultured in Dulbecco's modified Eagle's medium (DMEM) supplemented with 10% fetal bovine serum (FBS), 100 U penicillin, and 0.1 mg/mL streptomycin. U87ΔEGFR cells were prepared and maintained as described previously [12]. Cilengitide (EMD121974) was generously provided by Merck KgaA (Darmstadt, Germany) and the Cancer Therapy Evaluation Program, National Cancer Institute, National Institutes of Health. Bevacizumab was provided by Genentech (San Francisco, CA, USA) /Roche (Basel, Swiss) /Chugai Pharmaceutical Co (Tokyo, Japan).

Brain xenografts

All experimental animals were housed and handled in accordance with the guidelines of the Animal Research Committee of Okayama University. Before implantation, 85–90% confluent U87ΔEGFR cells were trypsinized, rinsed with DMEM supplemented with 10% FBS, and centrifuged at 100 × *g* for 5 min; the resulting pellet was resuspended in phosphate-buffered saline (PBS), and the cell concentration was adjusted to 1.0×10^5 cells/μL. U87ΔEGFR cells (5 μL) were injected into athymic rats (F344/N-rnu/rnu; CLEA Japan, Inc., Tokyo, Japan) and U87ΔEGFR cells (2 μL) were injected into athymic mice (balb/c-nu/nu; CLEA Japan, Inc, Tokyo, Japan). The animals were anesthetized and placed in stereotactic frames (Narishige, Tokyo, Japan) with their skulls exposed. Tumor cells were injected with a Hamilton syringe (Hamilton, Reno, NV, USA) into the right frontal lobe (in the athymic rats: 4 mm lateral and 1 mm anterior to the bregma at a depth of 4 mm; in the athymic mice: 3 mm lateral and 1 mm anterior to the bregma at a depth of 3 mm) and the syringe was withdrawn slowly after 5 min to prevent reflux. The skulls were then cleaned and the incision was sutured. PBS, bevacizumab (for the athymic mice and rats: 6 mg/kg), cilengitide (for the athymic mice and rats: 10 mg/kg), or a combination of bevacizumab and cilengitide of the same amount was administered 3 times/week intraperitoneally, starting on day 5 after tumor cell implantation.

Transmission electron microscopy

Athymic rats harboring U87ΔEGFR brain tumors were sacrificed at 18 days after tumor implantation and 6 times administration of PBS, bevacizumab, cilengitide, or the combination of bevacizumab and cilengitide. The brains were removed and fixed immediately by perfusion of 2% glutaraldehyde. After fixation in 2% osmium tetroxide, the samples were dehydrated and embedded in Spurr's resin. Thin sections poststained with salts of uranium and lead were cut to approximately 60 nm using an ultramicrotome (Leica EM UC6, Wetzlar, Germany). The samples were observed under a transmission electron microscopy (Hitachi H-7650 TEM, Tokyo, Japan).

Histopathological analysis of glioma

For histopathological analysis, athymic rats harboring U87ΔEGFR brain tumors were sacrificed at 18 days after tumor implantation. Athymic rats were anesthetized, euthanized by cardiac puncture, perfused with 100 mL PBS, and fixed with 50 mL 4% paraformaldehyde (PFA). The brains were removed and stored in 4% PFA for 12–24 h. Hematoxylin and eosin (HE) staining was performed as described previously [13]. For immunohistochemistry of PFA perfusion-fixed frozen sections, snap-frozen tissue samples were embedded in optimal cutting temperature compound for cryosectioning, and 16-μm thick sections were processed for indirect immunofluorescence. After blocking non-specific binding with 10% normal goat serum, the slides were incubated overnight at 4°C with primary antibodies, including those targeting rat endothelial cell antigen 1 (RECA-1) (1:20, mouse monoclonal; Abcam, Inc., Cambridge, UK), von Willebrand factor (1:250, rabbit polyclonal; Abcam, Inc., Cambridge, UK), integrin αvβ3 (1:100, mouse monoclonal; Abcam, Inc., Cambridge, UK), and integrin αvβ5 (1:75, mouse monoclonal; Abcam, Inc., Cambridge, UK), after blocking with 10% normal goat serum. After three washes with PBS containing 0.01% Tween 20 for 5 min, the slides were incubated with Alexa Fluor® 594-conjugated and Alexa Fluor® 488-conjugated secondary antibodies (Abcam, Inc., Cambridge, UK) and 4',6-diamidino-2-phenylindole (DAPI) (1:500) (Invitrogen, Carlsbad, CA, USA) in PBS for 60 min. The slides were then washed in PBS and mounted.

Microarray analysis

Orthotopic U87ΔEGFR xenograft mouse models treated with bevacizumab or the combination of bevacizumab and cilengitide were sacrificed at 18 days after tumor implantation (n = 3 per treatment). Approximately 40 mg of brain tumor samples were

excised cleanly from each mouse and RNA was extracted using TRIzol (Life Technologies, Carlsbad, CA, USA) and an RNeasy Mini Kit (QIAGEN, Venlo, Netherlands). They were analyzed using a CodeLink™ Human Whole Genome Bioarray (Applied Microarrays, Inc., Tempe, AZ, USA). We entrusted the microarray analyses to Filgen, Inc. (Nagoya, Japan). Briefly, for each bioarray, 10 μg of biotin-labeled aRNA, which was prepared using a MessageAmp™ II-Biotin Enhanced Kit in a total volume of 25 μL, were added to 5 μL of 5× fragmentation buffer, which was then incubated at 94°C for 20 min. Thereafter, 10 μg fragmented cRNA, 78 μL hybridization buffer component A, and 130 μL hybridization buffer component B were added, and the final volume was brought up to 260 μL with water. The resultant hybridization reaction mixture was incubated at 90°C for 5 min, after which 250 μL were slowly injected into the input port of each array, and the ports were sealed with sealing strips. The bioarrays were incubated for 18 h at 37°C while shaking at 300 rpm. A consistent hybridization time was maintained for comparative experiments. Following the incubation, the bioarrays were washed with 0.75 TNT buffer (0.10 M Tris-HCl, pH 7.6, 0.15 M NaCl, 0.05% Tween 20) and incubated at 46°C for 1 h. Each slot of the small reagent reservoir was then filled with 3.4 mL Cy5-streptavidin working solution, and the array was incubated at 25°C for 30 min. Thereafter, the bioarrays were washed 4 times for 5 min each with 1 × TNT buffer at 25°C, rinsed twice in 0.1× SSC (Ambion, Austin, TX, USA)/0.05% Tween 20 for 30 s each, and immediately dried by centrifugation for 3 min at 25°C. Finally, the arrays were scanned using a GenePix4000B Array Scanner (Molecular Devices, Sunnyvale, CA, USA). A gene was defined as being upregulated when the combination therapy/bevacizumab monotherapy average intensity ratio was >2.0, and downregulated when the combination therapy/bevacizumab monotherapy ratio was <0.5. We performed pathway analysis on the genes with increased and decreased expression using Microarray Data Analysis Tool Ver3.2 (Filgen, Inc., Nagoya, Japan). The data were extracted using the following criteria: Z-score > 0 and P-value < 0.05.

Quantitative reverse-transcription polymerase chain reaction (QRT-PCR)

Total RNA was isolated from cultured U87ΔEGFR cells treated with cilengitide (1.0 μM for 16 h) and untreated control U87ΔEGFR cells using an RNeasy® Mini Kit (QIAGEN, Hilden, Germany). *In vivo*, total RNA was extracted from the brain tumor tissue of mice that had been treated with PBS or cilengitide using the TRIzol reagent (Invitrogen, Carlsbad, CA, USA) according to the manufacturer's instructions. RNA was reverse transcribed with oligo dT primers using the SuperScript III First-Strand

Synthesis System for RT-PCR (Invitrogen, Carlsbad, CA, USA) according to manufacturer's instructions. Primers specific to each gene were designed using Primer 3 Plus Software (http://www.bioinformatics.nl/cgi-bin/primer3plus/primer3plus.cgi) and synthesized by Invitrogen. The resulting cDNA was amplified by PCR using the gene-specific primers and the 7300 Real Time PCR system (Applied Biosystems, Foster City, CA, USA) and a QuantiTectTM SYBR® Green PCR Kit (QIAGEN, Hilden, Germany). A log-linear relationship between the amplification curve and quantity of cDNA in the range of 1–1000 copies was observed. The cycle number at the threshold was used as the threshold cycle (Ct). Changes in the expression of mRNA were detected from 2-ΔΔCt using the 7300 Real Time PCR System with Sequence Detection Software (version 1.4; Applied Biosystems, Foster City, CA, USA). The amount of cDNA in each sample was normalized to the crossing point of the housekeeping gene glyceraldehyde 3-phosphate dehydrogenase (GAPDH). The following thermal cycling parameters were used: denaturation at 95°C for 10 min followed by 45 cycles at 94°C for 15 s, 55°C for 30 s, and 72°C for 30 s. The relative upregulation of mRNA for each gene in the control was calculated using their respective crossing points with the following formula, as previously described [14]:

$F = 2^{(TH - TG) - (OH - OG)}$ where, F = fold difference, T = control, O = treated cell or tumor, H = housekeeping gene (GAPDH), and G = gene of interest.

c-src tyrosine kinase primers:

CSK F (forward), 5′-GAATACCTGGAGGGCAACAA-3′

CSK R (reverse), 5′-ATTCCGAAACTCCACACGTC-3′

caveolin 3 primers:

CAV3 F (forward), 5′-TTTGCCAAGAGGCAGCTACT-3′

CAV3 R (reverse), 5′-ACCCTTTACTGGAGCCACCT-3′

GAPDH primers:

GAPDH F (forward), 5′- GAGTCAACGGATTTGGTCGT-3′

GAPDH R (reverse), 5′-TTGATTTTGGAGGGATCTCG-3′

To assess the gene expression of caveolin 3 and c-src tyrosine kinase with QRT-PCR, athymic mice harboring U87ΔEGFR brain tumors were sacrificed at 18 days after tumor implantation. The tumor-bearing right hemispheres of the brains were excised and processed for RNA.

Statistical analysis

Student's *t* test was used to test for statistical significance. Data are presented as the

mean ± standard error. $P < 0.05$ was considered statistically significant. All statistical analyses were performed with the use of SPSS statistical software (version 20; SPSS, Inc., Chicago, IL, USA).

Results

Anti-angiogenic effect of bevacizumab

U87ΔEGFR orthotopic tumors proliferate with aggressive angiogenic growth (Figure 1A). Treatment with bevacizumab reduced angiogenesis in U87ΔEGFR orthotopic tumor tissues in the rat with a regression of tumor size (Figure 1B). The density of tumor vessels was significantly decreased by bevacizumab (Figure 1C). The short diameter of tumor vessels tended to be larger, but there was no significant difference (Figure 1D). Quantitative assessment of tumor vascularity results in a remarkable regression of tumor vessels (Figure 1E).

Microstructure of tumor vessels in the border area with bevacizumab treatment

The structure of the blood-brain barrier of cerebral capillaries was composed of a single endothelial cell, juxtaposing membranes with a tight junction, pericytes attached to the abluminal surface of endothelial cells, a basal lamina surrounding these cells, and close contact with the plasma membranes of astrocyte end-feet [15]. We observed that there was no space between the basal lamina and astrocyte end-feet (AE) for capillaries in the contralateral normal brain (Figure 2A). The fuzzy basal lamina and loose ECM were observed at perivascular space in the center area of an untreated U87ΔEGFR tumor (see Supplementary Figure 1A). In the center area of a bevacizumab-treated U87ΔEGFR tumor, ECM was thickened and numerous collagen fibers were increased at perivascular space (see Supplementary Figure 1B). In contrast, there was a distance of more than 250 nm between endothelial cells and tumor cells and there was also a fuzzy basal lamina near the border area of the tumor (Figure 2B). When treated with bevacizumab, the distance between the endothelial cells and tumor cells was reduced in conjunction with the normalization and orderliness of the basal lamina (Figure 2C, D).

Anti-angiogenic therapy induced an invasive phenotype in the orthotopic glioma model

The rat orthotopic glioma model implanted with U87ΔEGFR cells displayed angiogenic growth and well-defined borders toward the brain tissue (Figure 3A). However, after anti-VEGF therapy with bevacizumab, we observed increased cell invasion and vascular

co-option (Figure 3B).

Integrin αvβ3 and αvβ5 expression in glioma cell lines

Using immunohistochemistry, we demonstrated that U87ΔEGFR cells expressed high levels of αvβ3 and αvβ5 integrin (Figure 4A, B). Furthermore, integrin αvβ3 and αvβ5 was immunohistochemically expressed at tumor endothelial cells and surrounding tumor cells in the rat orthotopic glioma model with U87ΔEGFR cells (Figure 4C, D). Therefore, we examined the combined effect of the integrin inhibitor cilengitide and bevacizumab on glioma models *in vivo*.

Effect of cilengitide on bevacizumab-induced invasion

The rat orthotopic glioma model with U87ΔEGFR cells die at approximately 20 days after implantation. Tumors in the untreated group were strongly proliferative and expanded with well-defined borders (Figure 5A). When treated with bevacizumab, the tumor surface became irregular, and strong invasiveness was induced in the U87ΔEGFR model (Figure 5B). Thus, when this model was treated with a combination of bevacizumab and cilengitide, the depth of tumor invasion was remarkably decreased (Figure 5C and D). These results demonstrated that cilengitide reduced bevacizumab-induced invasion.

Effects on the structure of tumor vessels by combination treatment with bevacizumab and cilengitide

We also focused on the effect of combination therapy with anti-VEGF and anti-integrin agents on tumor vessels. The vascularity of tumors treated with bevacizumab and cilengitide was strongly suppressed (Figure 6A). Similar to bevacizumab-treated tumors, cluttered and dense ECM around endotherial cells following combination therapy was observed by a transmission electron microscopy (see Supplementary Figure 1C). Notably, the tumor vessels around the area of the tumor border retained an orderly structured basal lamina (Figure 6B and C). Although the density of tumor vessels following combination therapy was inhibited to the same extent as with bevacizumab monotherapy (Figure 6D), the diameter of tumor vessels following combination therapy was significantly smaller than following bevacizumab monotherapy (Figure 6E). Additionally, vascularity of tumors following combination therapy was significantly less than that of bevacizumab-treated tumors (Figure 6F).

Microarray analysis of the effect of combination treatment compared to bevacizumab

monotherapy on the U87ΔEGFR orthotopic mouse model

To characterize the molecular mechanisms underlying the anti-invasive response to combination therapy, we analyzed the changes in gene expression of tumor tissues in the U87ΔEGFR orthotopic mouse model treated with bevacizumab and cilengitide combination therapy compared to bevacizumab monotherapy. We identified 947 differentially expressed genes between bevacizumab-treated U87ΔEGFR glioma tissue and bevacizumab plus cilengitide-treated U87ΔEGFR glioma tissue, which consisted of 486 upregulated genes and 461 downregulated genes (Figure 7A). Further, we characterized the functional significance of these dysregulated genes using pathway analysis. For the downregulated genes, the following three significantly enriched pathways were identified: *integrin-mediated cell adhesion pathway*, *signaling of hepatocyte growth factor (HGF) receptor pathway*, and *GPCRs, class C metabotropic glutamate, pheromone pathway* (Table 1). For the upregulated genes, the following three significantly enriched pathways were identified: *inflammatory response pathway*, s*erotonin receptor 2 and ELK-SRF-GATA4 signaling pathway*, and s*erotonin receptor 4-6-7 and NR3C signaling pathway* (Table 2).

Validation of the microarray results

To confirm the reliability of the results from the microarray analysis, caveolin 3 and c-src tyrosine kinase, which were included in the *integrin-mediated cell adhesion pathway* and associated with tumor invasion, were verified by QRT-PCR analysis. The relative expression of caveolin 3 and c-src tyrosine kinase in the U87ΔEGFR mouse orthotopic model treated with cilengitide and bevacizumab was significantly reduced compared with bevacizumab monotherapy by 0.38-fold and 0.44-fold, respectively ($p < 0.05$) (Figure 7B).

Discussion

Tumor angiogenesis in the glioma orthotopic models was decreased by treatment with bevacizumab. Conversely, bevacizumab treatment resulted in enhanced tumor invasion. In this study, we demonstrated that cilengitide, an inhibitor of these integrins, inhibited bevacizumab-induced glioma invasion *in vivo*. Microarray analysis of combination treatment compared to bevacizumab monotherapy on the U87ΔEGFR orthotopic mouse model showed that pathways such as the *integrin-mediated cell adhesion pathway* or *signaling of HGF receptor pathway* were associated with the anti-invasive mechanism of cilengitide. Moreover, we focused on the ultra-micro structure of tumor vessels.

Since a tight junction was maintained between the endothelial cells, disintegration of a basal lamina was considered to represent a broken blood-brain barrier. This observation revealed that bevacizumab increased perivascular ECM such as collagen fibers in the central area of the tumor and closed the normal blood-brain barrier with an orderly ECM wall in the border area of the tumor. Adding cilengitide further reduced the number of tumor vessels with a normalized blood-brain barrier at the border of the tumor.

The conditional approval of bevacizumab by the US Food and Drug Administration in 2009 for patients with recurrent glioblastoma was linked to future demonstrations of its efficacy in prospective trials of newly diagnosed patients. Two such trials were performed, largely in parallel—one by RTOG (RTOG-0825) and one by Roche (AVAGlio) [16]. At the 2013 ASCO meeting in Chicago, the results from both trials were shown to provide a uniform picture: progression-free survival was significantly prolonged, and quality of life was preserved in the AVAGlio trial, but not in RTOG-0825. Safety and tolerability were acceptable, but overall survival was not improved.

Several reports mentioned that increased tumor invasiveness is a major refractory to the antiangiogenic therapy. de Groot et al. described 3 patients who, during bevacizumab therapy, developed infiltrative lesions visible by MRI and presented the data that pair imaging features seen on MRI with histopathologic findings [17]. Delay et al. revealed hyperinvasive phenotype, which was one of resistance patterns of glioblastoma after bevacizumab therapy, was upregulated with *integrin signaling pathway* including integrin α5 and fibronectin 1 [18]. Our results also showed bevacizumab treatment led to increased cell invasion in spite of decreased angiogenesis.

Previous reports showed integrin αvβ3 and αvβ5 plays a central role in glioma invasion and inhibition of integrins decreased glioma cell motility *in vitro* [19,20]. We reported that cilengitide exerts its anti-tumor effects by inhibiting tumor angiogenesis and invasion or by inducing apoptosis-related pathways [9,13,21]. We recently established two novel invasive animal glioma models (J3T-1 and J3T-2) that reflect the invasive phenotype of human malignant gliomas [22]. These models were particularly beneficial to investigate the anti-invasive effects of cilengitide [13]. Currently, cilengitide is being assessed in phase II and phase III trials for patients with newly diagnosed glioblastoma [11,23]. Lombardi et al. recently reported two cases with bevacizumab-refractory high-grade glioma treated with cilengitide [24].

Some recent reports proved that the inhibition of VEGF promoted glioma invasion through HGF-dependent MET phosphorylation in association with phenotypic changes

such as the epithelial to mesenchymal transition [25,26]. The present study demonstrated that an antagonist of αvβ3 and αvβ5 integrin prevented bevacizumab-induced invasion in orthotopic glioma models that expressed these integrins at high levels. In the microarray analysis, combination therapy had reduced expression of genes in the *integrin-mediated cell adhesion pathway* and *signaling of HGF receptor pathway* compared to bevacizumab monotherapy. These data may indicate the mechanisms underlying the anti-invasive effects of cilengitide on glioma.

We showed that bevacizumab and cilengitide reduced tumor vascularity by changing the diameter and density of tumor vessels in the *in vivo* glioma models. Von Baumgarten et al. reported that bevacizumab decreased vascular density and normalized the vascular permeability of glioma [27]. Conversely, cilengitide was shown to shrink the diameter of tumor vessels in angiogenesis-dependent invasive glioma models [13]. Moreover, we investigated the ultra-micro structure of tumor vessels and proved that bevacizumab reduced the distance between endothelial cells and tumor cells with a broken basal lamina at the blood-brain barrier in the border of the tumor. We also focused the ECM of gliomas which is considered to play as a critical regulator of angiogenesis and invasiveness [28]. In the center area of U87ΔEGFR tumors following bevacizumab treatment and combination therapy of bevacizumab and cilengitide, ECMs were thickened remarlably at perivascular space with respectively different characteristics. Fibronectin, vitronectin, laminin, tenascin, and different types of collagen promote invasion of glioma [29,30], in contrast, glycosylated chondroitin sulfate proteoglycans consisting ECMs inhibit invasion in glioma [31]. These different mechanisms might be necessary for the regulation of tumor angiogenesis and invasion; however, the detailed mechanisms have not been elucidated and they need to be clarified in the future.

Conclusions

This study showed that anti-VEGF therapy induced glioma invasion despite its intense anti-angiogenic effect; however, the combination of bevacizumab with the αvβ3 and αvβ5 integrin inhibitor cilengitide exerted a significant anti-invasive effect. We revealed that combination therapy suppressed the *integrin-mediated cell adhesion pathway* as an underlying mechanism of its anti-invasive effect.

Acknowledgments

We thank M. Furutani, M. Arao, and N. Uemori for their technical assistance. The following medical students also contributed to the animal experiments: K. Fukumoto and N. Hayashi. Cilengitide was generously provided by Merck KgaA and the Cancer Therapy Evaluation Program, the National Cancer Institute, National Institutes of Health. Bevacizumab was generously provided by Genentech/Roche/Chugai Pharmaceutical Co. This study was supported by grants-in-aid for Scientific Research from the Japanese Ministry of Education, Culture, Sports, Science, and Technology to K.K. (No. 20890133; No. 21791364), and T.I. (No. 19591675; No. 22591611).

Conflict of interest

None of the authors have any conflicts of interest to declare.

Figure legends

Figure 1

Anti-angiogenic effect of bevacizumab

(A) Tumor vessels identified with RECA-1. Untreated U87ΔEGFR orthotopic tumor was observed with angiogenic growth. (B) The reduction of tumor vessels with bevacizumab therapy. Quantitative assessment of tumor vessels between no treatment and bevacizumab therapy was shown in following graphs. (C) Bevacizumab decreased vessel density of tumors significantly. (D) There was no significant difference about vessel short diameter of tumors. (E) Intensity of vessel area stained with RECA-1 was significantly reduced in bevacizumab-treated tumors. Bar: 100 μm. *$p < 0.01$. HPF, high power field.

Figure 2

Microstructure of tumor vessels in the border area with bevacizumab treatment

(A) Contralateral normal brain. There was no space between the basal lamina and astrocyte end-feet (AE) (black arrowheads). (B) There was a distance of more than 250 nm around the tumor microvessels; the fuzzy basal lamina and tumor cytoplasm (white arrowheads and double-headed black arrows) were separated in the border area of untreated U87ΔEGFR tumors. Conversely, a tight junction (white arrows) was maintained between the endothelial cells. (C) There was less space between the basal lamina and AE in the border area of bevacizumab-treated tumors compared to untreated tumors. (D) The distance between the endothelial cells and tumor was significantly narrowed in bevacizumab-treated tumors (Bev) compared to PBS-treated tumors (PBS). L: Lumen of vessels, Bar: 1 μm. *$p < 0.01$.

Figure 3

Anti-angiogenic therapy induces invasion in the orthotopic glioma model

(A) Well-defined borders toward the brain tissue in an untreated U87ΔEGFR orthotopic rat tumor. (B) Tumor cell invasion with vascular co-option in a bevacizumab-treated tumor. Bar: 100 μm.

Figure 4

Expression of integrin αvβ3 and αvβ5 in the glioma cell line

U87ΔEGFR cells expressed (A) αvβ3 and (B) αvβ5 integrin at a high level, especially αvβ3, in immunocytochemistry. (C) Integrin αvβ3 and (D) αvβ5 were expressed at a

high level in tumor vessels stained with von Willbrand factor and surrounding tumor cells in U87ΔEGFR rat orthotopic tumors. Bar: 50 μm.

Figure 5

The effect of cilengitide on bevacizumab-induced invasion

(A) HE staining of an untreated U87ΔEGFR rat orthotopic tumor demonstrated the expansion of the tumor with well-defined borders. (B) Following treatment with bevacizumab (Bev), the tumor border was irregular with tumor invasion. (C) Tumor invasiveness was reduced at the tumor border following combination therapy with bevacizumab and cilengitide (Bev+Cile) compared to bevacizumab monotherapy. (D) The depth of tumor invasion following treatment with bevacizumab and cilengitide was remarkably decreased compared to bevacizumab monotherapy. Bar: 200 μm. *$p < 0.01$.

Figure 6

Effects of combination treatment with bevacizumab and cilengitide on tumor vessel structure

(A) The tumor vessels treated with bevacizumab and cilengitide were inhibited more strongly than with bevacizumab treatment. Bar: 100 μm. (B) (C) Tumor vessels around the tumor border area retained an orderly structured basal lamina. L: Lumen of vessels, Bar: 5 μm. (D) The tumor vessel density following combination therapy (Bev+Cile) was inhibited to the same extent as with bevacizumab treatment (Bev), and the tumor vessel diameter was significantly smaller with combination therapy than with bevacizumab treatment (E). (F) Intensity of RECA-1 following combination therapy (Bev+Cile) was significantly less than that of bevacizumab-treated tumors. *$p < 0.05$. HPF, high power field.

Figure 7

Microarray analysis of the effect of combination treatment compared to bevacizumab monotherapy

(A) There were 947 differentially expressed genes between the bevacizumab monotherapy group (Bev) and the group with bevacizumab and cilengitide combination therapy (Bev+Cile), with 486 upregulated genes and 461 downregulated genes. (B) (C) Caveolin 3 (CAV3) and c-src tyrosine kinase (CSK) were significantly decreased by combination therapy compared to monotherapy (*$p < 0.05$) (mean ± SE, $n = 3$). RQ, relative quantification.

Supplementary Figure 1

Microstructure of perivascular space in the center area of U87ΔEGFR rat brain tumor

(A) The fuzzy basal lamina and loose ECM were observed at perivascular space in the center area of an untreated U87ΔEGFR tumor. (B) Numerous collagen fibers were increased at perivascular space in the center area of a bevacizumab-treated U87ΔEGFR tumor. (C) Cluttered and dense ECM around endotherial cells following combination therapy was observed. Bar: 500 nm.

Tables

Table 1

0.5-fold downregulated genes (n = 461)

Pathway Name	Z score	P-value	Entrez Gene ID	Gene Symbol	Gene Name
Integrin-Mediated Cell Adhesion	3.753	0.00398	6654	**SOS1**	son of sevenless homolog 1 (Drosophila)
	3.753	0.00398	859	**CAV3**	caveolin 3
	3.753	0.00398	1445	**CSK**	c-src tyrosine kinase
	3.753	0.00398	5747	**PTK2**	PTK2 protein tyrosine kinase 2
	3.753	0.00398	53358	**SHC3**	SHC (Src homology 2 domain containing) transforming protein 3
	3.753	0.00398	1793	**DOCK1**	dedicator of cytokinesis 1
Signaling of Hepatocyte Growth Factor Receptor	3.604	0.015347	6654	**SOS1**	son of sevenless homolog 1 (Drosophila)
	3.604	0.015347	5747	**PTK2**	PTK2 protein tyrosine kinase 2
	3.604	0.015347	1793	**DOCK1**	dedicator of cytokinesis 1
GPCRs, Class C Metabotropic Glutamate, Pheromone	3.725	0.026514	55507	**GPRC5D**	G protein-coupled receptor, family C, group 5, member D
	3.725	0.026514	846	**CASR**	calcium-sensing receptor

Table 2

2.0-fold upregulated genes (n = 486)

Pathway Name	Z score	P-value	Entrez Gene ID	Gene Symbol	Gene Name
Inflammatory Response Pathway	3.473	0.017558	3913	**LAMB2**	laminin, beta 2 (laminin S)
	3.473	0.017558	3560	**IL2RB**	interleukin 2 receptor, beta
	3.473	0.017558	958	**CD40**	CD40 molecule, TNF receptor superfamily member 5
Serotonin Receptor 2 and ELK-SRF-GATA4 Signaling	3.375	0.034361	5604	**MAP2K1**	mitogen-activated protein kinase kinase 1
	3.375	0.034361	2776	**GNAQ**	guanine nucleotide binding protein (G protein), q polypeptide
Serotonin Receptor 4-6-7 and NR3C Signaling	3.121	0.041792	5604	**MAP2K1**	mitogen-activated protein kinase kinase 1
	3.121	0.041792	673	**BRAF**	v-raf murine sarcoma viral oncogene homolog B1

References

Journal Articles

[1] Stupp R, Mason WP, van den Bent MJ, Weller M, Fisher B, Taphoorn MJ, Belanger K, Brandes AA, Marosi C, Bogdahn U, et al. (2005). Radiotherapy plus concomitant and adjuvant temozolomide for glioblastoma. *N Engl J Med* **352**, 987-996.

[2] Bokstein F, Shpigel S, and Blumenthal DT (2008). Treatment with bevacizumab and irinotecan for recurrent high-grade glial tumors. *Cancer* **112**, 2267-2273.

[3] Vredenburgh JJ, Desjardins A, Herndon JE, 2nd, Marcello J, Reardon DA, Quinn JA, Rich JN, Sathornsumetee S, Gururangan S, Sampson J, et al. (2007). Bevacizumab plus irinotecan in recurrent glioblastoma multiforme. *J Clin Oncol* **25**, 4722-4729.

[4] Dvorak HF (2002). Vascular permeability factor/vascular endothelial growth factor: a critical cytokine in tumor angiogenesis and a potential target for diagnosis and therapy. *J Clin Oncol* **20**, 4368-4380.

[5] Desjardins A, Reardon DA, Herndon JE, 2nd, Marcello J, Quinn JA, Rich JN, Sathornsumetee S, Gururangan S, Sampson J, Bailey L, et al. (2008). Bevacizumab plus irinotecan in recurrent WHO grade 3 malignant gliomas. *Clin Cancer Res* **14**, 7068-7073.

[6] Piao Y, Liang J, Holmes L, Zurita AJ, Henry V, Heymach JV, and de Groot JF (2012). Glioblastoma resistance to anti-VEGF therapy is associated with myeloid cell infiltration, stem cell accumulation, and a mesenchymal phenotype. *Neuro Oncol* **14**, 1379-1392.

[7] Hynes RO (2002). Integrins: bidirectional, allosteric signaling machines. *Cell* **110**, 673-687.

[8] Maubant S, Saint-Dizier D, Boutillon M, Perron-Sierra F, Casara PJ, Hickman JA, Tucker GC, and Van Obberghen-Schilling E (2006). Blockade of alpha v beta3 and alpha v beta5 integrins by RGD mimetics induces anoikis and not integrin-mediated death in human endothelial cells. *Blood* **108**, 3035-3044.

[9] Onishi M, Kurozumi K, Ichikawa T, Michiue H, Fujii K, Ishida J, Shimazu Y, Chiocca EA, Kaur B, and Date I (2013). Gene expression profiling of the anti-glioma effect of Cilengitide. *Springerplus* **2**, 160.

[10] Oliveira-Ferrer L, Hauschild J, Fiedler W, Bokemeyer C, Nippgen J, Celik I, and Schuch G (2008). Cilengitide induces cellular detachment and apoptosis in endothelial and glioma cells mediated by inhibition of FAK/src/AKT pathway. *J Exp Clin Cancer Res* **27**, 86.

[11] Kurozumi K, Ichikawa T, Onishi M, Fujii K, and Date I (2012). Cilengitide treatment for malignant glioma: current status and future direction. *Neurol Med Chir (Tokyo)* **52**, 539-547.

[12] Kambara H, Okano H, Chiocca EA, and Saeki Y (2005). An oncolytic HSV-1 mutant expressing ICP34.5 under control of a nestin promoter increases survival of animals even when symptomatic from a brain tumor. *Cancer Res* **65**, 2832-2839.

[13] Onishi M, Ichikawa T, Kurozumi K, Fujii K, Yoshida K, Inoue S, Michiue H,

Chiocca EA, Kaur B, and Date I (2013). Bimodal anti-glioma mechanisms of cilengitide demonstrated by novel invasive glioma models. *Neuropathology* **33**, 162-174.

[14] Kurozumi K, Hardcastle J, Thakur R, Yang M, Christoforidis G, Fulci G, Hochberg FH, Weissleder R, Carson W, Chiocca EA, et al. (2007). Effect of tumor microenvironment modulation on the efficacy of oncolytic virus therapy. *J Natl Cancer Inst* **99**, 1768-1781.

[15] Hawkins BT and Davis TP (2005). The blood-brain barrier/neurovascular unit in health and disease. *Pharmacol Rev* **57**, 173-185.

[16] Weller M and Yung WK (2013). Angiogenesis inhibition for glioblastoma at the edge: beyond AVAGlio and RTOG 0825. *Neuro Oncol* **15**, 971.

[17] de Groot JF, Fuller G, Kumar AJ, Piao Y, Eterovic K, Ji Y, and Conrad CA (2010). Tumor invasion after treatment of glioblastoma with bevacizumab: radiographic and pathologic correlation in humans and mice. *Neuro Oncol* **12**, 233-242.

[18] DeLay M, Jahangiri A, Carbonell WS, Hu YL, Tsao S, Tom MW, Paquette J, Tokuyasu TA, and Aghi MK (2012). Microarray analysis verifies two distinct phenotypes of glioblastomas resistant to antiangiogenic therapy. *Clin Cancer Res* **18**, 2930-2942.

[19] Platten M, Wick W, Wild-Bode C, Aulwurm S, Dichgans J, and Weller M (2000). Transforming growth factors beta(1) (TGF-beta(1)) and TGF-beta(2) promote glioma cell migration via Up-regulation of alpha(V)beta(3) integrin expression. *Biochem Biophys Res Commun* **268**, 607-611.

[20] Deryugina EI and Bourdon MA (1996). Tenascin mediates human glioma cell migration and modulates cell migration on fibronectin. *J Cell Sci* **109 (Pt 3)**, 643-652.

[21] Fujii K, Kurozumi K, Ichikawa T, Onishi M, Shimazu Y, Ishida J, Chiocca EA, Kaur B, and Date I (2013). The integrin inhibitor cilengitide enhances the anti-glioma efficacy of vasculostatin-expressing oncolytic virus. *Cancer Gene Ther*.

[22] Inoue S, Ichikawa T, Kurozumi K, Maruo T, Onishi M, Yoshida K, Fujii K, Kambara H, Chiocca EA, and Date I (2011). Novel Animal Glioma Models that Separately

Exhibit Two Different Invasive and Angiogenic Phenotypes of Human Glioblastomas. *World Neurosurg*.

[23] Onishi M, Kurozumi K, Ichikawa T, and Date I (2013). Mechanisms of Tumor Development and Anti-angiogenic Therapy in Glioblastoma Multiforme. *Neurol Med Chir (Tokyo)*.

[24] Lombardi G, Zustovich F, Farina P, Polo V, Farina M, Puppa AD, Bertorelle R, Gardiman MP, Berti F, and Zagonel V (2012). Cilengitide in bevacizumab-refractory high-grade glioma: two case reports and critical review of the literature. *Anticancer Drugs* **23**, 749-753.

[25] Lu KV, Chang JP, Parachoniak CA, Pandika MM, Aghi MK, Meyronet D, Isachenko N, Fouse SD, Phillips JJ, Cheresh DA, et al. (2012). VEGF inhibits tumor cell invasion and mesenchymal transition through a MET/VEGFR2 complex. *Cancer Cell* **22**, 21-35.

[26] Piao Y, Liang J, Holmes L, Henry V, Sulman E, and de Groot JF (2013).

Acquired Resistance to Anti-VEGF Therapy in Glioblastoma Is Associated with a Mesenchymal Transition. *Clin Cancer Res* **19**, 4392-4403.

[27] von Baumgarten L, Brucker D, Tirniceru A, Kienast Y, Grau S, Burgold S, Herms J, and Winkler F (2011). Bevacizumab has differential and dose-dependent effects on glioma blood vessels and tumor cells. *Clin Cancer Res* **17**, 6192-6205.

[28] Ziu M, Schmidt NO, Cargioli TG, Aboody KS, Black PM, and Carroll RS (2006). Glioma-produced extracellular matrix influences brain tumor tropism of human neural stem cells. *J Neurooncol* **79**, 125-133.

[29] Mahesparan R, Read TA, Lund-Johansen M, Skaftnesmo KO, Bjerkvig R, and Engebraaten O (2003). Expression of extracellular matrix components in a highly infiltrative in vivo glioma model. *Acta Neuropathol* **105**, 49-57.

[30] Huijbers IJ, Iravani M, Popov S, Robertson D, Al-Sarraj S, Jones C, and Isacke CM (2010). A role for fibrillar collagen deposition and the collagen internalization receptor endo180 in glioma invasion. *PLoS One* **5**, e9808.

[31] Silver DJ, Siebzehnrubl FA, Schildts MJ, Yachnis AT, Smith GM, Smith AA, Scheffler B, Reynolds BA, Silver J, and Steindler DA (2013). Chondroitin sulfate proteoglycans potently inhibit invasion and serve as a central organizer of the brain tumor microenvironment. *J Neurosci* **33**, 15603-15617.

Figures

Figure 1

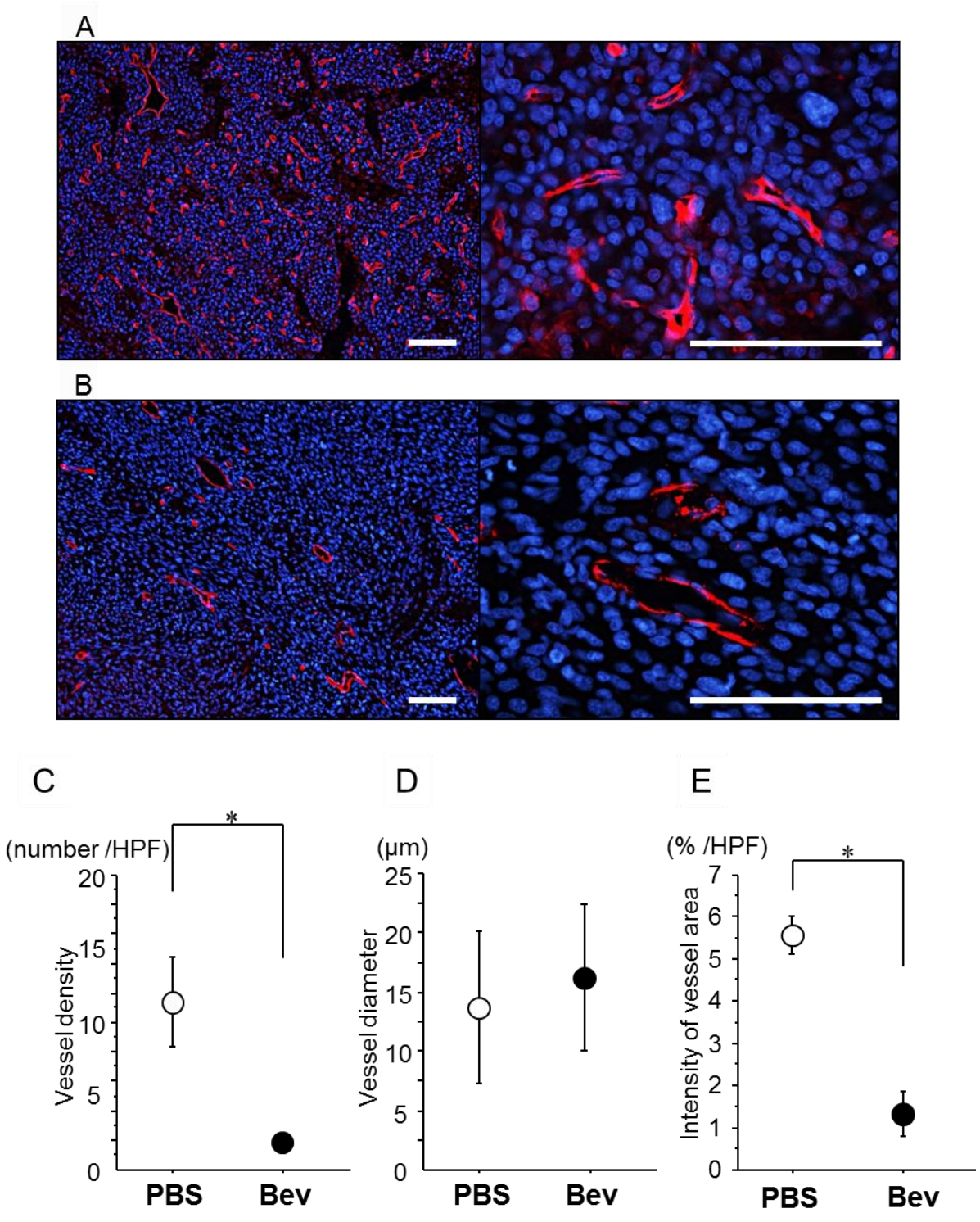

Figure 2

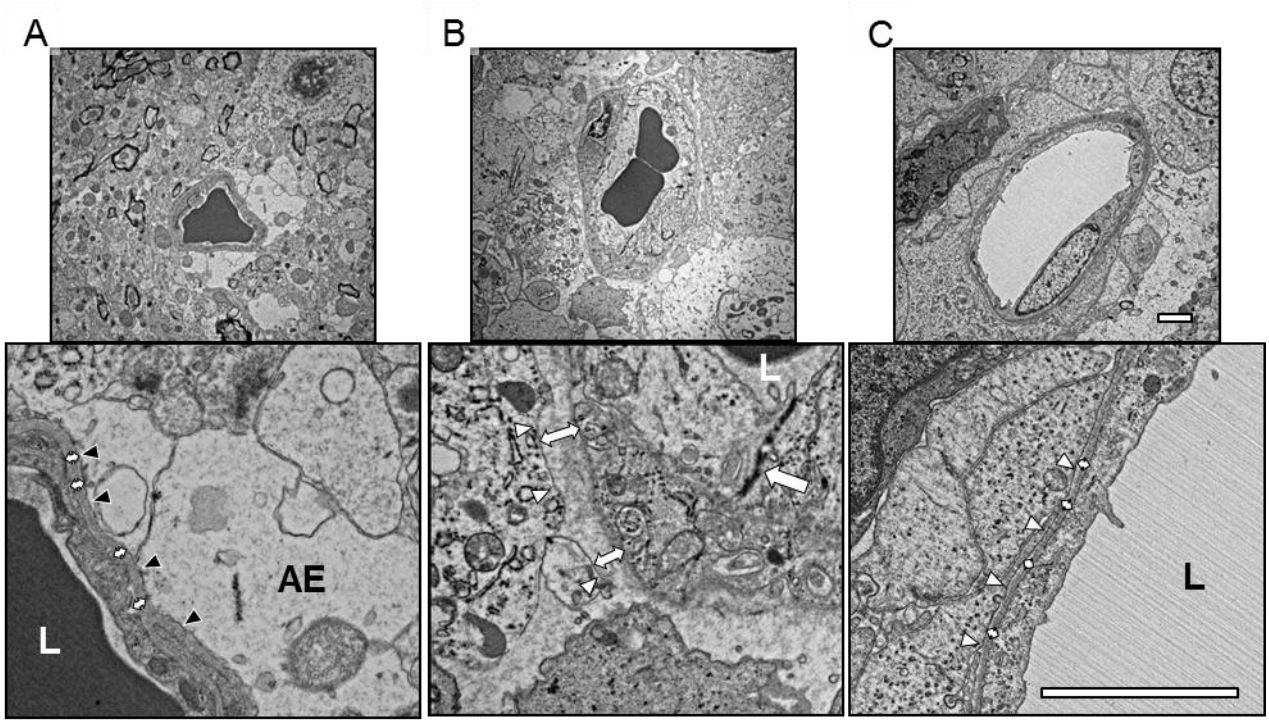
A
B
C
AE
L
L
L

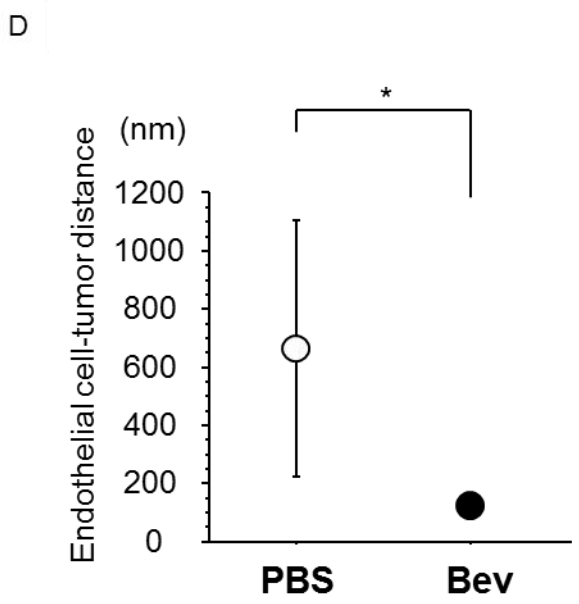
D
*
(nm)
Endothelial cell-tumor distance
1200
1000
800
600
400
200
0
PBS
Bev

Figure 3

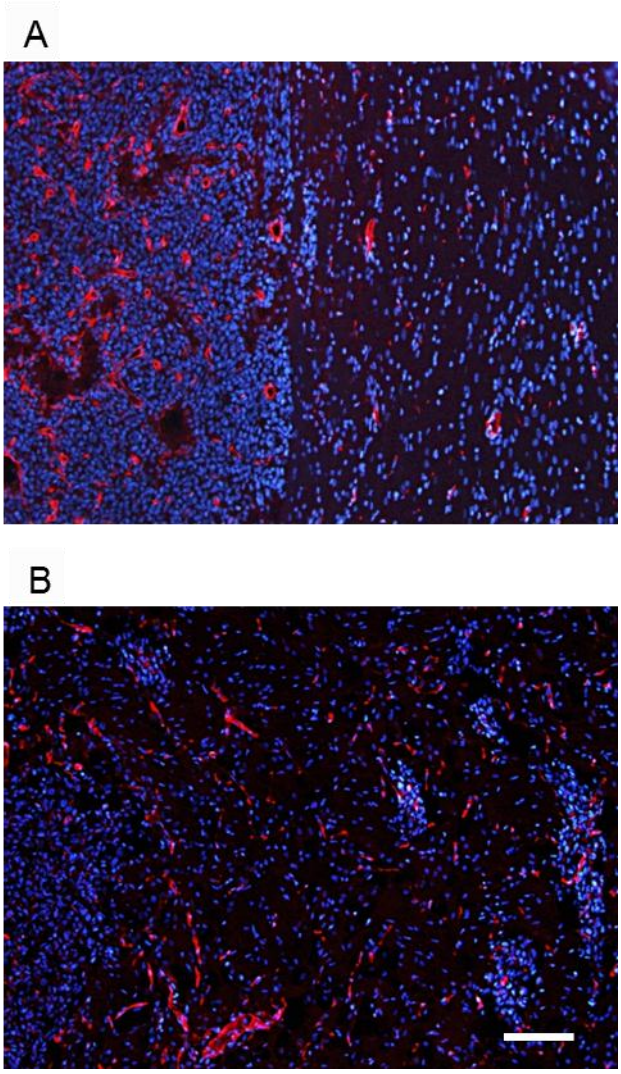

Figure 4

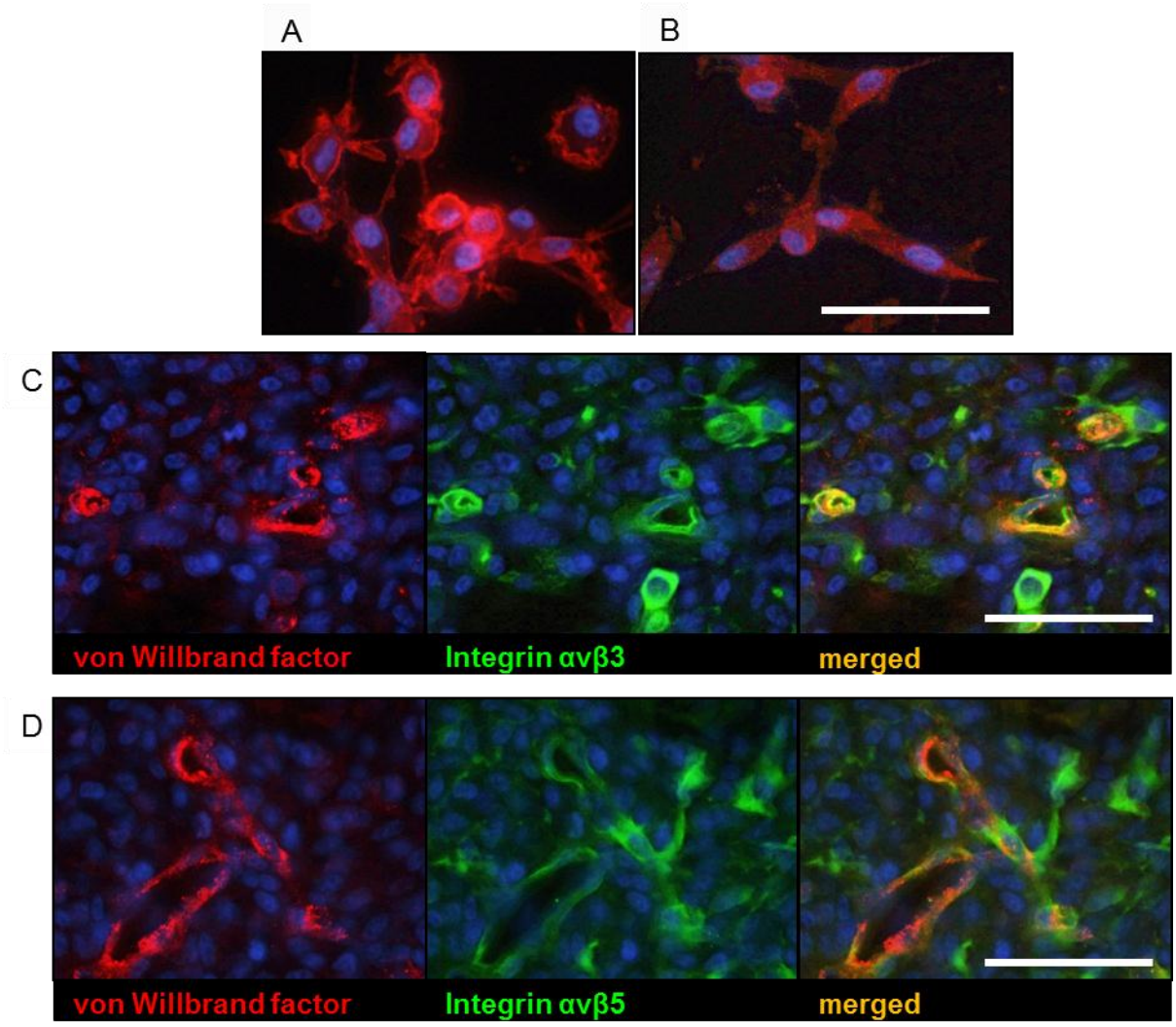
A
B
C
von Willbrand factor
Integrin αvβ3
merged
D
von Willbrand factor
Integrin αvβ5
merged

Figure 5

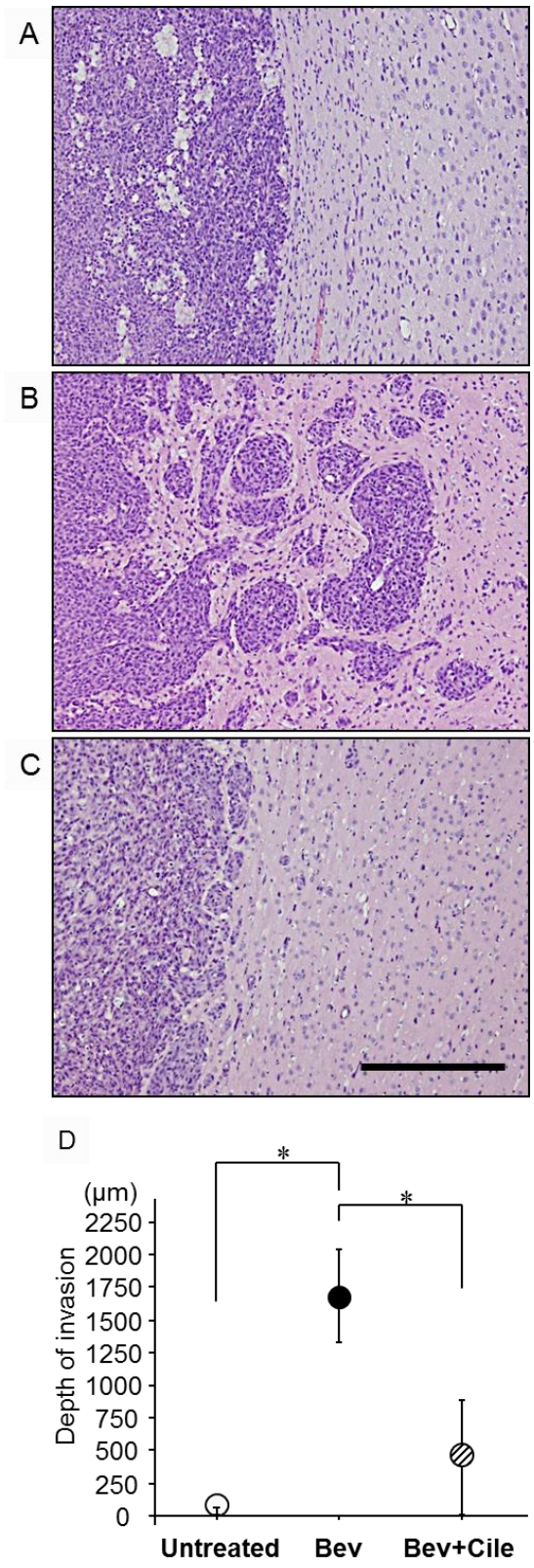
A
B
C
D
*
*
(μm)
2250
2000
1750
1500
1250
1000
750
500
250
0
Depth of invasion
Untreated
Bev
Bev+Cile

Figure 6

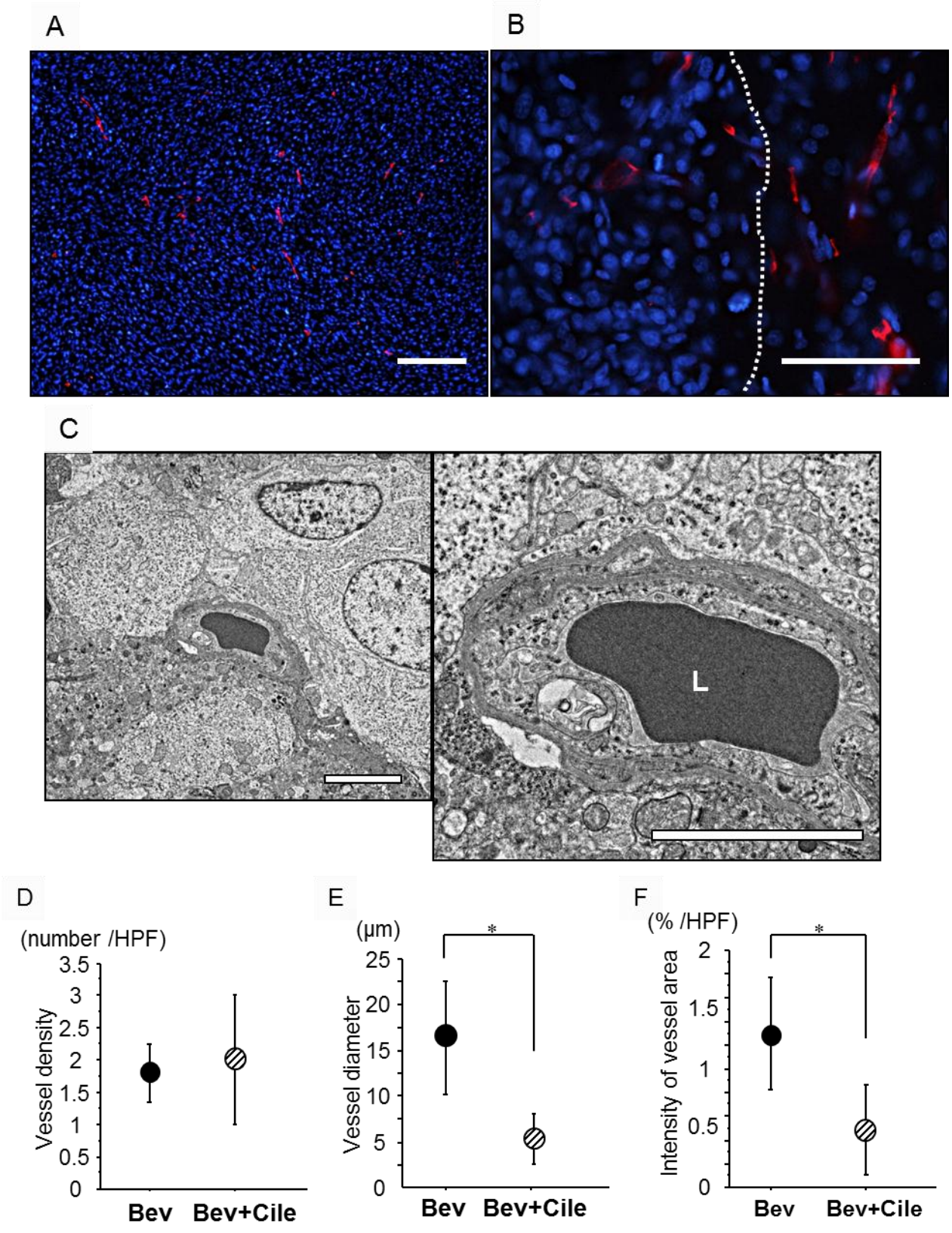
A
B
C
L
D
(number /HPF)
Vessel density
3.5
3
2.5
2
1.5
1
0.5
0
Bev
Bev+Cile
E
(μm)
Vessel diameter
25
20
15
10
5
0
*
Bev
Bev+Cile
F
(% /HPF)
Intensity of vessel area
2
1.5
1
0.5
0
*
Bev
Bev+Cile

Figure 7

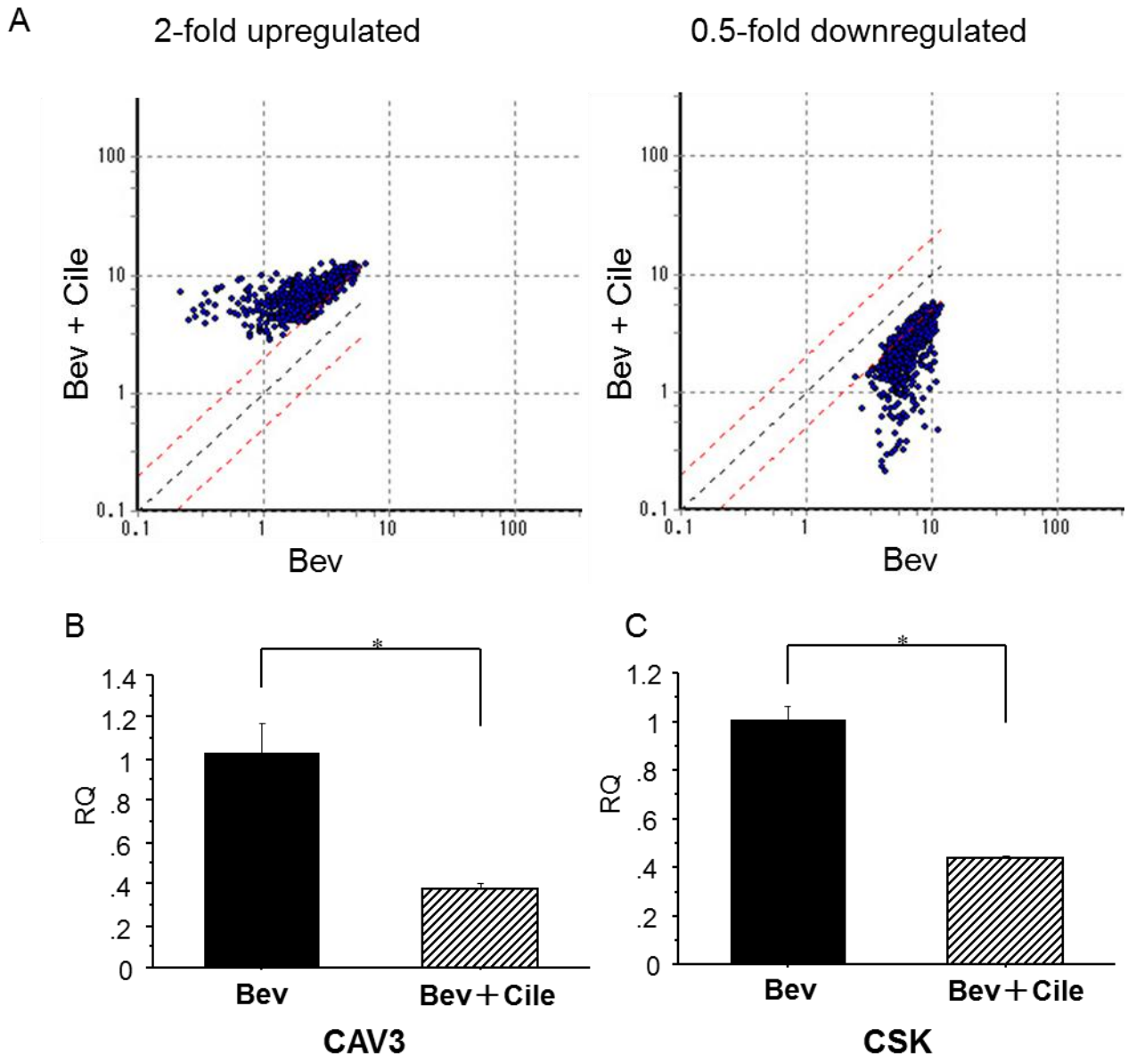
A
2-fold upregulated
0.5-fold downregulated
Bev + Cile
Bev
100
10
1
0.1
B
C
RQ
1.4
1.2
1
.8
.6
.4
.2
0
*
Bev
Bev+Cile
CAV3
CSK

Supplemental Data

Supplementary Figure 1